High-frequency EPR on high-spin transitions-metal sites

Mathies, G.

Chapter 5

High-frequency EPR study of the pseudo-tetrahedral high-spin Fe^{2+} complex $Fe[(SPPh_2)_2N]_2$

We report continuous-wave (cw) EPR spectra of a powder of the high-spin Fe^{2+} complex $Fe[(SPPh_2)_2N]_2$ at 275.7 GHz (J band) and 94.1 GHz (W band). These spectra show that the complex occurs in two different conformations, which have a slightly different electronic structure near the iron ion. At J band also crystals of the complex were studied, which made it possible to assign the signals observed in the powder spectra to the two slightly different iron sites and determine their spin-Hamiltonian parameters with high accuracy.

Guinevere Mathies, Spyros Chatziefthimiou, Dimitrios Maganas, Yiannis Sanakis, Silvia Sottini, Panayotis Kyritsis and Edgar J. J. Groenen, *in preparation.*

5.1 Introduction

Pursuit of experimental data on the electronic structure of high-spin Fe^{2+} sites is of great relevance for bioinorganic chemistry. [98, 113] High-spin Fe^{2+} occurs in the active sites of many metalloproteins, but the understanding of their electronic structure is still developing. [8] Electron-paramagnetic-resonance (EPR) spectroscopy is a suitable and sensitive method to investigate the electronic structure of paramagnetic transition-metal sites. However, high-spin Fe^{2+} systems, $S = 2$, tend to be EPR silent at the standard microwave frequency of 9.5 GHz (X band) or, if a spectrum is observed, it is little informative. [114–117]

The degeneracy of the five magnetic sublevels of the $S = 2$ spin system, a non-Kramers system, may be completely lifted at zero field. This zero-field splitting (ZFS) is often much larger than the X-band microwave quantum. Therefore the quantitative study of high-spin Fe^{2+} systems by EPR had to await the technical development of high-frequency/high-field EPR (HF EPR). [118] In recent literature a handful of studies of high-spin Fe^{2+} complexes by HF EPR can be found, [119–125] and one study of a frozen solution of the protein rubredoxin, which contains in the reduced form high-spin Fe^{2+} in its active site. [59]

Here we study the high-spin Fe^{2+} complex $Fe[(SPPh_2)_2N]_2$, abbreviated as $Fe^{Ph,Ph}L_2$, by high-frequency EPR. In this complex two bidentate disulfidoimidodiphosphinato ligands constitute a compressed, approximately tetrahedral sulfur coordination of the iron, see Figure 5.1.

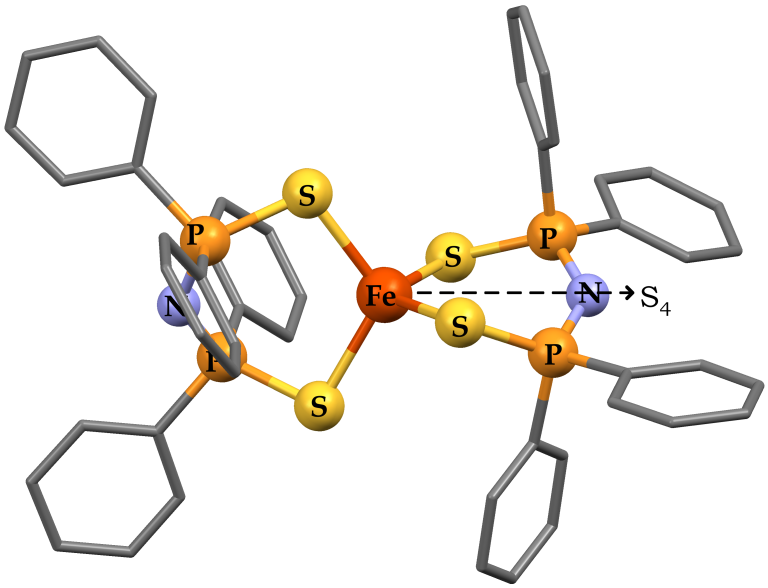

Figure 5.1: The molecular structure of $Fe[(SPPh_2)_2N]_2$.

We report continuous-wave (cw) EPR spectra of $Fe^{Ph,Ph}L_2$ powder at 275.7 GHz (J band) and 94.1 GHz (W band). These spectra show that the complex occurs in two different conformations, which have a slightly different electronic structure near the iron ion. At J band also crystals of the complex were studied, which made it possible to assign the signals observed in the powder spectra to the two slightly different iron sites and determine their spin-Hamiltonian parameters with high accuracy.

5.2 Materials and methods

5.2.1 Sample preparation

$Fe^{Ph,Ph}L_2$ was prepared as described by Davison et al. [126] Grain/crystal size was determined by the ratio CH_2-Cl_2/hexane from which the material was recrystallized, which determined the precipitation speed. The $Fe^{Ph,Ph}L_2$ crystals show variation in color. Some are brownish, others are colorless to the eye. The brownish crystals are suspected to contain a Fe^{3+} species. The quality of the crystals varies. Many, particularly the larger ones, consist of multiple crystals grown together. For the J-band crystal measurements high-quality, colorless crystals were selected. The crystals had a parallelepiped shape of which the length of two edges was similar and the third edge was considerably longer. The size of the crystals studied at J band was estimated to be $0.3 \times 0.08 \times 0.08$ mm. For the J-band experiments a suprasil sample tube of inner diameter 0.15 mm was used (VitroCom Inc.). The effective sample volume, determined by the microwave cavity, is approximately 20 nl. [64] The sample tube was filled with silicon grease to fix the crystal at low temperatures. To align the long edge of the crystal with the sample tube axis a crystal was stuck to a suprasil rod with silicon grease and inserted into the sample tube, which was filled with grease.

5.2.2 EPR experiments

The cw J-band EPR spectra were recorded on an in-house developed spectrometer, [9] using a probe head specialized for operation in cw mode as described in Chapter 2. [64] A single-mode cavity was used for detection of the EPR signal. A sample tube can be inserted from one end of the cavity and rotated by 360 degrees around its axis. The magnetic field is applied perpendicular to this axis. The cw W-band spectra were recorded on a Bruker Elexsys E680 spectrometer using a W-band "ENDOR" probe head with a cylindrical TE_{011} cavity in a CF935W flow cryostat (Oxford Instruments). During the low-temperature experiments the waveguide was heated just outside the cryostat to avoid condensation inside the waveguide. The cw X-band spectra were also recorded on a Bruker Elexsys E680 spectrometer, using a TE_{102} rectangular cavity equipped with an ESR 900 Cryostat (Oxford Instruments).

5.3 Results

Figure 5.2 shows the cw J-band spectra of a powder of $Fe^{Ph,Ph}L_2$ at 10, 25 and 50 K. The spectra are rich in signals and cover a magnetic field range of 10 T. A group of signals between 0.8 and 3.5 T loses intensity relative to a second group of four signals between 5.5 and 9 T as the temperature increases. As the magnetic field sweep starts from zero the EPR signal decreases, which suggests an absorption of microwaves at zero field, and reaches a minimum approximately at 700 mT at 10 K and approximately at 200 mT at 25 and 50 K. The fine structure, most pronounced in the 10 K spectrum around 2 T, which seems to be noise, reproduces in consecutive scans, but changes if the sample tube is rotated between scans.

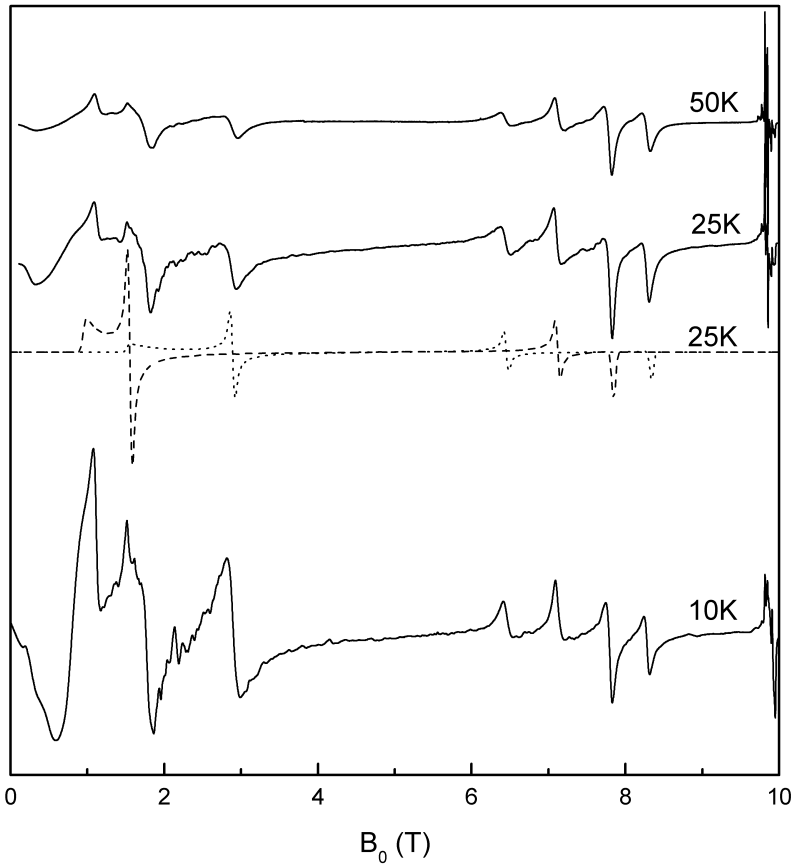

Figure 5.2: J-band powder spectra of $Fe^{Ph,Ph}L_2$ at 10, 25 and 50 K. Solid lines: experimental spectra, dashed line: simulation molecule 1, dotted line: simulation molecule 2. Experimental conditions: microwave frequency 275.7 GHz, microwave power 1 μW, modulation amplitude 3 mT, modulation frequency 1.8 kHz. Around $g = 2$ (9.84 T) signals from a Mn^{2+} impurity are observed.

In Figure 5.3 the J-band spectrum of a crystal of $Fe^{Ph,Ph}L_2$ shows a low-field group of signals and a high-field group of four signals. This crystal was placed in the sample tube such that its long edge was parallel to the axis of the sample tube, around which it can be rotated. The magnetic field is applied perpendicular to this axis of rotation. Figure 5.4 shows the behavior of the high-field signals as the sample is rotated. The four signals belong together two by two, as indicated in Figure 5.4 by the dashed and dotted lines. The dashed lines intersect at an orientation of 0 (and 90) degrees, while the dotted lines intersect at an orientation of 15 (and 105) degrees. Apart from a number of "extra" signals, marked in Figure 5.4, the high-field part of the J-band crystal spectrum is invariant under a rotation by 90 degrees. Spectra recorded on this crystal at 10 and 5 K showed no significant changes in the relative intensities of the four high-field signals, but the "extra" signals became relatively strong at 5 K.

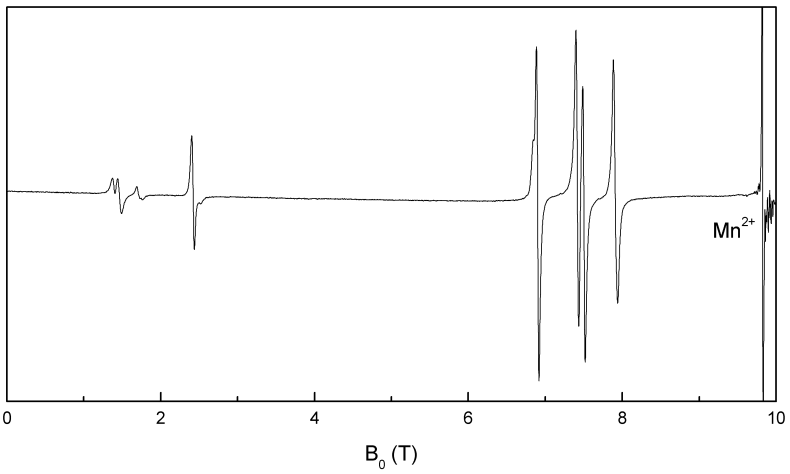

Figure 5.3: J-band spectrum at 25 K of a crystal of $Fe^{Ph,Ph}L_2$ aligned such that B_0 is approximately perpendicular to the long edge of the crystal. The relative orientation of the crystal in the plane perpendicular to the long crystal edge is 90 degrees, see Figure 5.4. Around $g = 2$ (9.84 T) signals from a Mn^{2+} impurity are observed.

Crystal spectra were also recorded at J band for two other crystals, one oriented arbitrarily and one aligned with its long edge perpendicular to the axis of the sample tube. Spectra of both crystals showed the low-field and high-field groups of signals, and the dependence on the orientation of the crystal with respect to the applied magnetic field in line with the spectra shown in Figure 5.3 and Figure 5.4. For the orientation of the long edge of the crystal parallel to the applied magnetic field the latter crystal showed a signal at 250 mT.

Spectra recorded at W band in cw mode for $Fe^{Ph,Ph}L_2$ powder show three signals, at 0.9, 1.4 and 2.9 T, see Figure 5.5. Also a very broad signal is observed, stretching

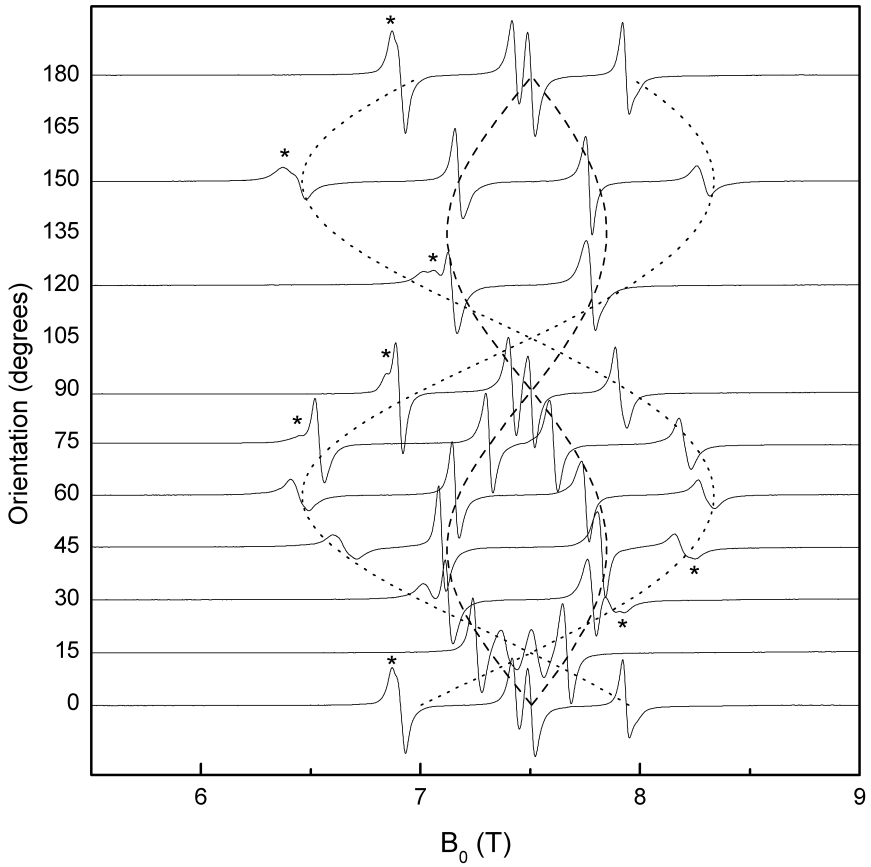

Figure 5.4: High-field region of J-band spectra at 25 K of a $Fe^{Ph,Ph}L_2$ crystal aligned such that B_0 is approximately perpendicular to the long edge of the crystal. The angles shown in the graph represent the relative orientation around the long crystal edge, the orientation of 0 degrees is chosen arbitrarily. The dashed and dotted lines show the behavior of the resonance fields calculated using EasySpin for molecule 1 and molecule 2, respectively, under the assumption that the z-axis of the spin system is perfectly perpendicular to B_0. The "extra" signals are marked with a $\star$.

from approximately 0.5 to 3.5 T, of which the exact shape is difficult to resolve due to baseline drift during the scan, and a sharp peak at 1.6 T. All signals become stronger if the temperature is lowered from 20 to 12.5 K.

Figure 5.6 shows X-band spectra of a powder of $Fe^{Ph,Ph}L_2$. A broad peak is observed, which shifts to lower field and broadens as the temperature increases. The maximum of the peak is observed at 67, 65.6, 62.2, 53.4 mT at 5, 20, 40, 60 K respectively.

J-band spectra were also measured on a diamagnetically diluted powder containing 5% $Fe^{Ph,Ph}L_2$ and 95% $Zn^{Ph,Ph}L_2$ and on a mixed crystal containing 1% $Fe^{Ph,Ph}L_2$

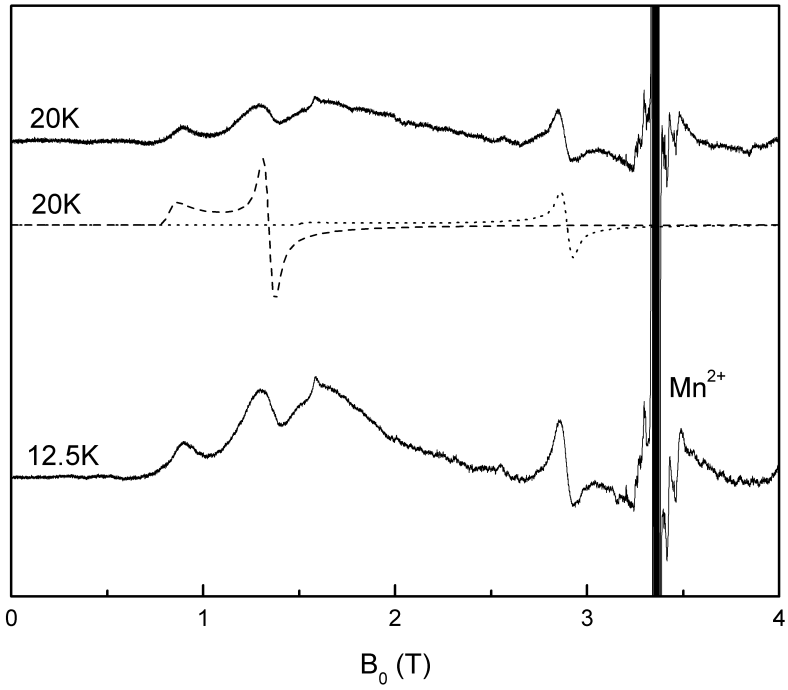

Figure 5.5: W-band powder spectra of $Fe^{Ph,Ph}L_2$ at 12.5 and 20 K. Solid lines: experimental spectra, dashed line: simulation molecule 1, dotted line: simulation molecule 2. Experimental conditions: microwave frequency 94.1 GHz, microwave power 0.02 mW, modulation amplitude 1.5 mT, modulation frequency 90 kHz. A strong Mn^{2+} impurity is observed at $g = 2$ (3.36 T). A baseline was subtracted.

and 99% $Zn^{Ph,Ph}L_2$. These spectra were in agreement with the 100% $Fe^{Ph,Ph}L_2$ spectra, and were of low intensity, according to the diamagnetic dilution. Attempts to detect an electron spin echo of 100% $Fe^{Ph,Ph}L_2$ powder at J band and W band were not successful, not even at 1.7 K.

5.4 Analysis

The EPR spectra of high-spin Fe^{2+}, $S = 2$, are interpreted using the following spin Hamiltonian. [3]

$$H = \mu_B \vec{B}_0 \cdot \vec{\vec{g}} \cdot \vec{S} + \vec{S} \cdot \vec{\vec{D}} \cdot \vec{S} \tag{5.1}$$

The g tensor in the first term describes the anisotropy of the Zeeman interaction. The second term is a field independent fine-structure term, the zero-field splitting (ZFS). The ZFS tensor, $\vec{\vec{D}}$, is symmetric, can be taken traceless, and is characterized

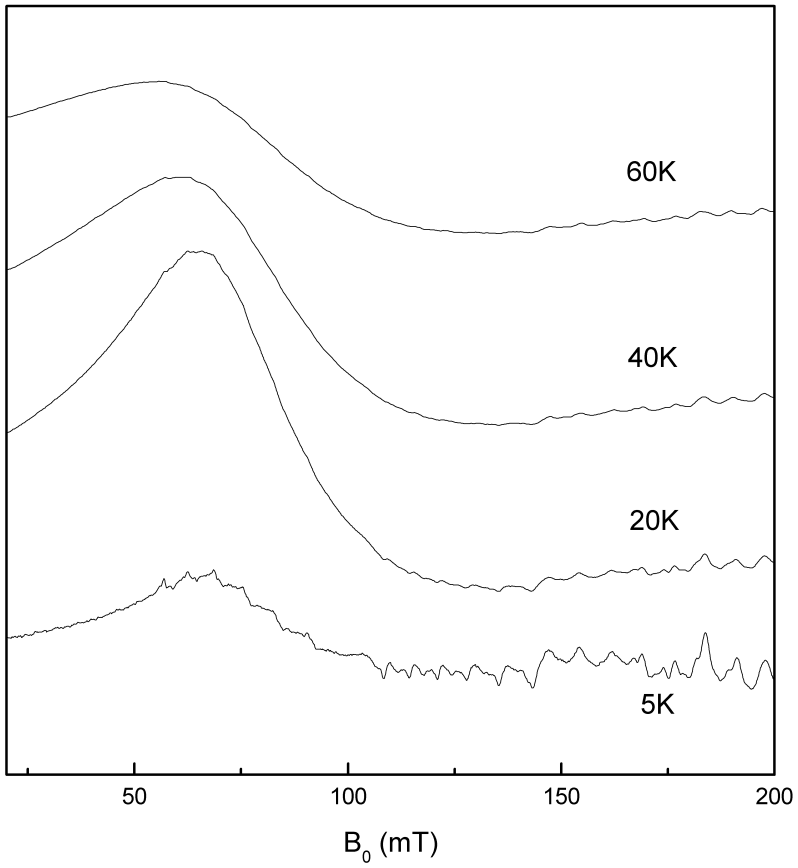

Figure 5.6: X-band powder spectra of $Fe^{Ph,Ph}L_2$ at 5, 20, 40 and 60 K. Experimental conditions: microwave frequency 9.488 GHz, microwave power 100 mW, modulation amplitude 0.5 mT, modulation frequency 100 kHz. The wiggles showing up in the 5 K spectrum most prominently are forbidden transitions of a Mn^{2+} impurity.

by two parameters, D and E.

$$D = 3/2D_z,\ E = 1/2(D_x - D_y) \tag{5.2}$$

The rhombicity of $\vec{\vec{D}}$ is given by the ratio $\lambda = E/D$. The principal axes are chosen such that $|D_z| > |D_y| > |D_x|$ and thus $0 < \lambda < 1/3$.

In zero field the eigenfunctions and eigenvalues of this spin Hamiltonian are [116]

$$\begin{aligned}
|2^{s'}\rangle &= \sqrt{\frac{1}{2}\left(1+\frac{D}{\sqrt{D^2+3E^2}}\right)}\frac{|+2\rangle+|-2\rangle}{\sqrt{2}} \\
&+ \sqrt{\frac{1}{2}\left(1-\frac{D}{\sqrt{D^2+3E^2}}\right)}|0\rangle \\
|2^{a}\rangle &= \frac{1}{\sqrt{2}}\left(|+2\rangle-|-2\rangle\right) \\
|1^{s}\rangle &= \frac{1}{\sqrt{2}}\left(|+1\rangle+|-1\rangle\right) \\
|1^{a}\rangle &= \frac{1}{\sqrt{2}}\left(|+1\rangle-|-1\rangle\right) \\
|0'\rangle &= \sqrt{\frac{1}{2}\left(1-\frac{D}{\sqrt{D^2+3E^2}}\right)}\frac{|+2\rangle+|-2\rangle}{\sqrt{2}} \\
&+ \sqrt{\frac{1}{2}\left(1+\frac{D}{\sqrt{D^2+3E^2}}\right)}|0\rangle
\end{aligned} \tag{5.3}$$

$$\begin{aligned}
E_{2s'} &= 2\sqrt{D^2+3E^2} \\
E_{2a} &= 2D \\
E_{1s} &= -D+3E \\
E_{1a} &= -D-3E \\
E_{0'} &= -2\sqrt{D^2+3E^2}
\end{aligned} \tag{5.4}$$

The size of $|D|$ is typically between 150 and 600 GHz. If the ZFS tensor is axial, $\lambda = 0$, the quintet splits into two doublets, $|2^{s'}\rangle$, $|2^{a}\rangle$ and $|1^{s}\rangle$, $|1^{a}\rangle$, and a singlet, $|0'\rangle$. A non-zero value of λ lifts the degeneracy completely and introduces an $m_s = 0$ component in the $|2^{s'}\rangle$ state and $m_s = \pm 2$ components in the $|0'\rangle$ state, as shown by the accent in the names of the states. For $D > 0$ the state $|0'\rangle$ is the lowest in energy.

Figure 5.7 shows the behavior of the five magnetic sublevels as a function of B_0 applied along the principal directions x, y and z for a positive D of 266 GHz and $\lambda = 0.052$, assuming that the principal axes of the D and g tensor are collinear. These ZFS parameters describe one of the two molecules present in the $Fe^{Ph,Ph}L_2$ samples we investigated, as will become clear in this section. J-band transitions are shown in Figure 5.7 by vertical lines. From the temperature dependence of their intensity we conclude that the low-field signals observed in the J-band spectra arise from transitions from the ground state $|0'\rangle$ to the states $|1^{s}\rangle$, $|1^{a}\rangle$, while the high-field

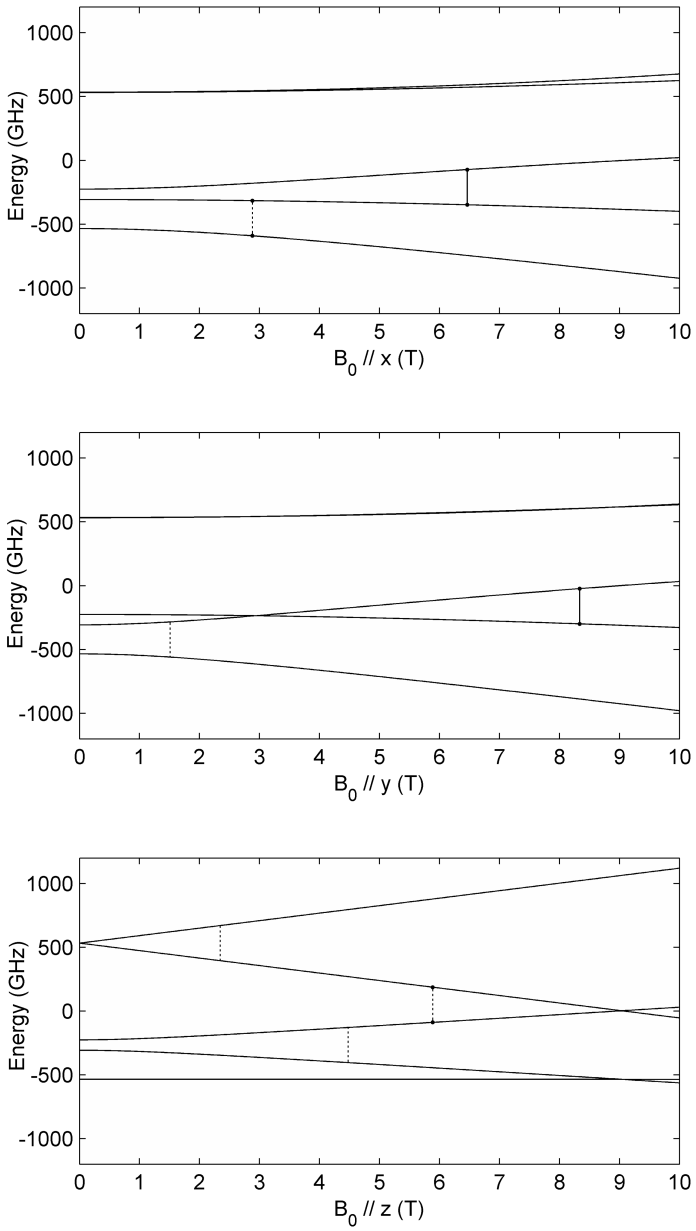

Figure 5.7: The dependence of the energy of the five magnetic sublevels of the $S = 2$ spin system on the magnitude of the magnetic field applied along the x, y and z direction for molecule 2. The vertical lines show 275.7 GHz resonances. The dashed resonances have a low transition probability.

signals arise from transitions between the states $|1^s\rangle$ and $|1^a\rangle$. We will start with the interpretation of the high-field signals.

At high magnetic fields the states $|1^s\rangle$ and $|1^a\rangle$ start to behave almost as a doublet. The powder spectrum of an anisotropically split doublet reflects the principal values of the g tensor. In this case a 275.7 GHz transition within the "$|1^s\rangle$, $|1^a\rangle$ doublet" is almost forbidden if B_0 is parallel to the z-axis of the system and the powder spectrum is expected to show only the transitions drawn in the energy level plots for $B_0 \parallel x$ at 6.4 T and $B_0 \parallel y$ at 8.3 T. However, the J-band spectra of $Fe^{Ph,Ph}L_2$ show four signals in the range $5.5 - 9$ T, not two. There are no signs of an exchange interaction between the iron sites, which could additionally split the energy levels, since the spectra on the diamagnetically diluted material match the 100% $Fe^{Ph,Ph}L_2$ spectra. This suggests that there are two $Fe^{Ph,Ph}L_2$ molecules with slightly different spin-Hamiltonian parameters contributing to the powder spectra.

The crystal spectra recorded at J band help to separate the signals contributing to the powder spectra. The behavior of the high-field signals as the crystal is rotated around an axis parallel to its long edge and perpendicular to B_0 is shown in Figure 5.4. Clearly the inner signals, see the dashed lines in Figure 5.4, and the outer signals, see the dotted lines, belong together. The extreme resonance fields of the two outer signals, as in the spectra of relative orientation 60 and 150 degrees, correspond to the two outer high-field signals in the powder spectrum shown in Figure 5.2. Thus, the long edge of the crystal must be parallel to the z-axis of the spin system, of which the behavior of the magnetic sublevels is plotted in Figure 5.7. Rotation around the axis of the sample tube corresponds to a rotation in the x, y-plane. The inner signals arise from what we call molecule 1 and the outer signals arise from molecule 2. The x,y-axes of molecule 1 are rotated around the common z-axis by approximately 15 degrees with respect to the x,y-axes of molecule 2.

Each crystal spectrum in Figure 5.4 shows four high-field signals, which is remarkable, since two signals, one from each molecule, are expected. Also, a rotation by 90 degrees returns the same spectrum. This can only be explained if both molecules occupy two magnetically distinguishable sites, which are rotated with respect to each other by 90 degrees around the z-axis.

To determine the spin-Hamiltonian parameters that describe the electronic structure of the iron sites of the two molecules, the experimental J-band spectra were compared to spectra calculated by numerical diagonalization of the spin-Hamiltonian using EasySpin. [6] Starting values for the ZFS parameters D and E were determined from the J-band powder spectra, using the information we obtained from the crystal spectra, namely that the two inner high-field signals arise from molecule 1 and the two outer high-field signals arise from molecule 2. These two parameter sets would give rise to W-band transitions between the states $|1^s\rangle$ and $|1^a\rangle$. The exact resonance fields of these transitions are very sensitive to the value of E and therefore the signals observed at 0.9, 1.4 and 2.9 T in the W-band powder spectra were used to establish the value of E for both parameter sets. Further fine tuning was performed from the J-band powder spectra, which are very sensitive to D and the principal values of the g tensor.

The spin-Hamiltonian parameters that describe the iron sites of the two molecules best are

$$\begin{aligned}(\mathbf{1}) \quad & D = 275 \text{ GHz},\ \lambda = 0.021 \\ & g_x = 2.11,\ g_y = 2.14,\ g_z = 2.1 \\ (\mathbf{2}) \quad & D = 266 \text{ GHz},\ \lambda = 0.052 \\ & g_x = 2.10,\ g_y = 2.12,\ g_z = 2.1\end{aligned}$$

Powder spectra calculated with these parameters are shown in Figure 5.2 and Figure 5.5, taking into account an isotropic line width of 50 mT. In Figure 5.4 the calculated behavior of the high-field resonances in the x, y-plane is shown for both parameter sets. From the dependence of the J- and W-band resonances on a change in the parameters, as calculated using EasySpin, we estimate the uncertainties in the spin-Hamiltonian parameters: ± 2 GHz for D, ± 0.002 for λ, ± 0.01 for g_x, g_y, and ± 0.05 for g_z.

The X-band $Fe^{Ph,Ph}L_2$ powder spectra show a peak that shifts to lower field as the temperature is increased, starting at 67 mT at 5 K. This resonance is incompatible with the parameter sets 1 and 2. In an X-band spectrum molecule 2 is expected to show a weak positive peak at 90 mT resulting from a transition between the states $|2^{s'}\rangle$ and $|2^{a}\rangle$. Molecule 1 has an almost axial ZFS tensor, which makes a transition between $|2^{s'}\rangle$ and $|2^{a}\rangle$ forbidden, and is not expected to give any signal at X-band. We conclude that the observed X-band spectra do not arise from molecules 1 and 2, which gave rise to the dominant features in the J- and W-band spectra. Moreover, the two parameter sets do not cover the microwave absorption at zero field in the J-band powder spectrum and the broad signal between 0.5 and 3.5 T and the sharp peak at 1.6 T in the W-band powder spectra. In the crystal spectra shown in Figure 5.4 we observed "extra" resonances and in the J-band spectrum of the crystal aligned with its long edge parallel to B_0 we observed a signal at 250 mT. These observations point to the presence of a third component with a conformation that is not well defined in the powder. For this component the spin-Hamiltonian parameters are distinctly different from those for molecules 1 and 2, and we estimate $D \approx 210$ GHz and $\lambda \approx 0.1$.

5.5 Discussion

The low-field and high-field groups of signals observed in the J-band spectra of $Fe^{Ph,Ph}L_2$ powder, see Figure 5.2, and also the signals observed in the W-band powder spectra at 0.9, 1.4, 2.9 T, see Figure 5.5, can be understood with the parameter sets 1 and 2. The signals observed in the crystal spectra at J band and their dependence on the relative orientation of B_0 are covered, see Figure 5.4. Small deviations in the calculated resonance fields and, for some orientations, small, unexpected splittings

of the resonances are observed, because we did not attempt to align the principal x and y axes of the spin system exactly with B_0.

The resonance fields of a J-band spectrum of a typical high-spin Fe^{2+} system are sensitive to a small change in the spin-Hamiltonian parameters, as is clear from the error estimates in these parameters. For our system the W-band resonances were sensitive to a change in E, but rather insensitive to a change in the other parameters, which made it possible to use these spectra as a starting point in the fine tuning of the parameters. The spectra of the crystal were necessary to distinguish between the two components present in the powder spectra.

The shapes of the resonances are not as well reproduced by the simulations as the resonance fields. For instance, the line width of the low-field signals in the J-band powder spectra can not be properly reproduced. More importantly, the shape of the four high-field signals in the J-band powder spectra is not properly calculated. In fact, for unknown reasons, already in the simulations of the crystal spectra the intensity of the high-field transitions, which arise if B_0 is parallel, or nearly parallel, to the y-axis, is underestimated. This mismatch between experiment and simulation deserves further attention.

The signals in the experimental spectra that are not covered by the parameter sets 1 and 2 arise from a third component, which is distinctly different from molecule 1 and 2. The width of the zero-field resonance in the J-band powder spectra and the extremely broad peak in the W-band powder spectra suggest that there is a distribution of conformations this component can take up in the powder. The presence of such a distribution can explain the shift of the positive peak in the X-band spectra to lower field as the temperature is increased. As the values of D and E change, both the resonance field of the transition between the states $|2^{s'}\rangle$ and $|2^{a}\rangle$ and the temperature at which its intensity is highest shift.

Figure 5.1 shows the structure of $Fe^{Ph,Ph}L_2$ as determined by X-ray diffraction on a crystal at room temperature (S. Chatziefthimiou, private communication). The FeS_4 core assumes an approximately compressed tetrahedral geometry (two larger angles, 115°, and four smaller ones, 107°). [95] The bidentate $(SPPh_2)_2N$ ligands form two twisted rings with the iron atom. The complex as a whole has approximately S_4 symmetry.

The complex $Fe^{Ph,Ph}L_2$ crystallizes in the P_{-1} space group. The edges of the unit cell are 14.364(7), 13.823(6) and 13.337(6) Å, the angles α, β and γ are 110.203(16), 114.032(17) and 82.425(13) degrees, respectively. The unit cell contains two molecules, which are connected by an inversion center and therefore can not be distinguished by EPR. The J-band and W-band EPR spectra of $Fe^{Ph,Ph}L_2$ powder, however, can only be explained by, at least, two sets of spin-Hamiltonian parameters, which undoubtedly arise from, at least, two molecules, which differ in structure. Moreover, in the crystal these two molecules are found to occur at two magnetically distinguishable sites, which are rotated with respect to each other by 90 degrees around the z-axis. Thus, the EPR spectra of $Fe^{Ph,Ph}L_2$ are incompatible

with the information obtained on the crystal structure by X-ray diffraction.

X-ray diffraction on a crystal of the analogous $Co^{Ph,Ph}L_2$ complex revealed a unit cell, space group P_{-1}, that contains in total four molecules. [127] Molecule 1a and 2a are crystallographically independent and are connected to molecule 1b and 2b by an inversion center. Two molecules with different spin-Hamiltonian parameters are thus expected to be observed by EPR spectroscopy. However, only one set of spin-Hamiltonian parameters was observed experimentally. [5] X-ray diffraction on crystals of the analogous $Zn^{Ph,Ph}L_2$ complex revealed two crystal structures, i.e. two different unit cells: one unit cell similar to the unit cell described above for $Fe^{Ph,Ph}L_2$ and another unit cell similar to the unit cell described above for $Co^{Ph,Ph}L_2$ (S. Kyritsis, private communication).

To assure that the unit cell of the crystal studied by J-band EPR is the unit cell described above for $Fe^{Ph,Ph}L_2$ and to exclude that the crystal we studied is a twin, X-ray diffraction was performed, at room temperature, on one of the crystals we studied at J band. This crystal was found to be a single crystal and, moreover, the unit cell is indeed the unit cell described above for $Fe^{Ph,Ph}L_2$. Thus, a remarkable incompatibility between the X-ray diffraction data and the EPR data on this material stands. Possibly the temperature at which the data are acquired plays a role: room temperature for X-ray diffraction versus 50 K or less for the EPR spectroscopy. Small temperature dependent variations in structure for high-spin Fe^{2+} complexes have been observed by others. [124, 125] We are currently investigating this possibility.

5.6 Conclusion

While X-band EPR spectra of high-spin Fe^{2+} systems are notoriously poor in information, the W-band and particularly the J-band EPR spectra of $Fe^{Ph,Ph}L_2$ are very rich and sensitive to small changes in the electronic structure of the iron sites. The combination of J-band and W-band EPR on this complex both in the form of a powder and of a crystal made it possible to determine with high accuracy the spin-Hamiltonian parameters of both conformations in which the complex occurs.